Simulation of Soft Clay Ground Improvement Using The Stone Column Method (Case Study: 10000m³ Storage Tank)

Muhamad Akbar Afriandi[1*] and Herwan Dermawan[1]
[1]Civil Engineering Study Program, Indonesia University of Education
*Corresponding Author: Muhamad Akbar Afriandi. Email: m.akbarafriandi@gmail.com

Abstract

This study evaluates the performance of soft clay soil improvement beneath a 10000 m³ cylindrical storage tank using stone columns equipped with load transfer platforms (LTP) through 3D numerical simulation in PLAXIS 3D. A quarter – domain model was constructed using Mohr – Coulomb material properties and a triangular grid scheme; the parametric study included column lengths L = 0, 3, 9, 17, 19, 25 m, replacement area ratio As = 25% and 35%, and column stiffness Ec = 35 and 70 MPa. The case without reinforcement shows a total settlement of approximately 0.388 m. After reinforcement, the settlement decreases nonlinearly with increasing L, As, and Ec, with a performance jump occurring when the column penetrates the entire thickness of the soft clay (17 m). At As = 35% and Ec = 70 MPa, the settlement becomes 0.147 m for L = 19 m (SIF around 2.64) and 0.139 m for L = 25 m (SIF around 2.79). Strain analysis shows a shift in mechanism from punching (short columns) to bulging (long columns), consistent with the increase in stress concentration ratio (SCR) at the column head, ranging from 3.5 to 5.35. The LTP thickness of approximately 1 m plays a role in widening load dispersion and reducing differential settlement between columns. These findings provide practical guidance for selecting L, As, and Ec to meet the service limits of tanks on soft clay.

Keywords: Stone Column, Soft Clay, Settlement, Settlement Improvement Factor, Stress Concentration, Stress Concentration Ratio, Numerical Study

1. INTRODUCTION

Large – scale infrastructure development, such as a 10000 m^3 storage tank on soft clay soil, is a challenge that continues to be faced in Indonesia. Approximately 20 million hectares, or more than 10% of Indonesia's land area, is covered by soft soil, making issues such as low strength, high compressibility, significant deformation, and low permeability real reliability concerns for structures built on top of it. These conditions require effective soil improvement solutions to ensure the stability and performance of structures throughout their operational lifespan.

Among various methods, stone columns (SC) are widely used because they can increase soil mass stiffness, reduce effective compressibility, and improve pore water pressure dissipation pathways. For extensive area loads such as tanks, the performance of the soil – column system is influenced by several key design decisions, including the column length (L) relative to the thickness of the soft layer, the replacement area ratio (As) reflecting the column diameter – spacing, and the column material stiffness (Ec) resulting from compaction. At the same time, the deformation mechanism of the columns can exhibit punching behavior in short columns and transition to bulging as the columns penetrate the soft layer, which further influences how the load is distributed between the columns and the soil.

Although SC usage is widespread, there are still gaps: (i) stress distribution in soil – column systems is complex; (ii) 2D unit cell numerical approaches are often insufficiently representative to capture column group interactions under extensive tank loads; and (iii) studies on design parameter variations in soft soil conditions in Indonesia are still limited. These gaps motivate the conduct of a 3D numerical study to map the influence of key design parameters on system performance.

Based on these issues, this study formulates three main questions: (1) what are the characteristics of settlement performance and deformation patterns of SC – reinforced soft soil; (2) what is the mechanism of load transfer from columns to the surrounding soil; and (3) what parameters most influence settlement performance, deformation patterns, and stress distribution in SC systems.

In line with this, the objectives of the study are: (1) to analyze the characteristics of settlement performance and post – reinforcement deformation patterns; (2) to analyze the load transfer mechanism in the SC system; and (3) to evaluate design parameters that significantly affect deformation performance and stress distribution. Practically, the study results are expected to provide more effective SC design recommendations to reduce settlement and improve the stability of tank structures on soft clay soils, as well as more representative stress concentration ratio values for local soil conditions.

2. METHOD

This study uses a quantitative descriptive research method that aims to describe and analyze phenomena occurring in soft clay soil repaired with stone columns, such as settlement performance, deformation patterns, and stress distribution. This method was chosen because the study focuses on numerical analysis of the influence of stone column design variables, such as area replacement ratio, column length, and material strength.

2.1. Objects, Geometry, and Soil Improvement Schemes

The object analyzed is a 10000 m^3 cylindrical storage tank erected on soft clay soil. The tank's operating load is represented as uniform pressure on the base with an intensity of approximately 87 kPa (including the self – weight component). The improvement system uses stone columns (SC) on a triangular grid covered by a granular load transfer platform (LTP) approximately 1.0 m thick directly beneath the tank base. The column diameter is taken as d = 1.2 m. Two replacement area ratios are analyzed: As = 25% and As = 35%. With the triangular grid, the equivalent spacing between columns (s) is approximately s = 2.30 m (As 25%) and s = 2.00 m (As 35%). Column lengths were varied as L = 0, 3, 9, 17, 19, 25 m to evaluate the effect of penetration relative to the thickness of the soft clay (17 m).

2.2. Numerical Modeling

Modeling was performed using PLAXIS 3D with a quarter domain model to take advantage of load symmetry and reduce computational costs. The boundary conditions on the symmetry plane were normal displacement restrictions (roller), while the base of the model was fully confined (ux = uy = uz = 0). The ground surface was free without constraints.

Material model. Soil and columns were modeled using Mohr – Coulomb; soil parameters were obtained from field correlations (NSPT) calibrated with local literature. Columns were treated as fully drained with a high effective friction angle (ϕ = 42 – 45°) and two column modulus levels (E_c = 35 MPa and 70 MPa). LTP is modeled as granular material (E = 50 – 60 MPa; ϕ = 38 – 40°). The explicit column – soil interface is not modeled, but the relative roughness effect is captured through the contrast in stiffness and friction angle.

Discretization & sensitivity. A 10 – node tetrahedral element mesh was used with local refinement at the column head and within the LTP to capture stress/strain gradients. Sensitivity tests showed global reduction variations < ~5% with mesh refinement and load steps, so the selected mesh was deemed adequate.

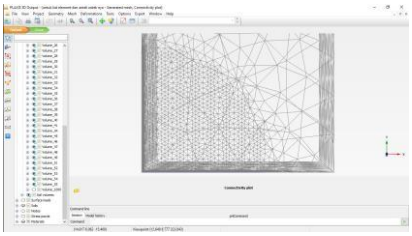

Fig. 1. Mesh Distribution
Source: Analysis Results

2.3. Parametric Study Matrix

In this analysis, several parameter values were used for parametric studies as shown in the Table 1: Parametric Study Matrix.

Table 1: Parametric Study Matrix

Parameter	Value
Area Replacement Ratio	25%, 35%
Panjang Stone Column	3m, 9m, 17m, 19m, 25m
Modulus, Ec	35 MPa, 70 MPa

Source: Analysis Results

2.4. Output Variables

There are several research outputs that are expected to be achieved in this study, including:

a) Settlement performance, in the form of evaluation of settlement improvement factor and total settlement.

b) Deformation pattern, in the form of identification of deformation patterns (bulging, punching, or combination) based on the distribution of settlement and strain that occurs.

c) Stress distribution, in the form of analysis of stress distribution in soil and stone columns, as well as obtaining the stress concentration ratio value.

3. Results and Discussion

3.1. Settlement Improvement Factor

The distribution of deflection in all scenarios shows a concave pattern with the maximum value at the center of the tank (Fig. 2). This pattern is consistent with the stress distribution on a circular load, so that the deflection gradually decreases toward the edges. At this stage, the baseline without repair results in $S_0 = 0.388$ m.

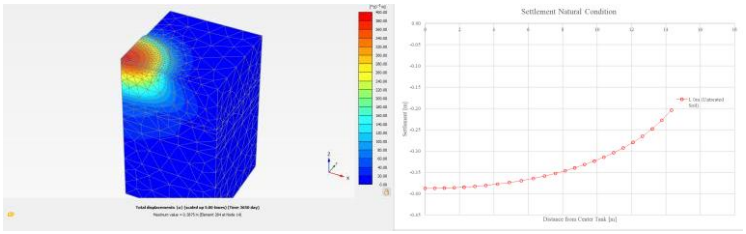

Fig. 2. Settlement Natural Condition (Unimproved Soil)
Source: Analysis Results

When the column length (L) is still shorter than the thickness of the soft clay (L < 17 m), the influence of As and Ec on the magnitude of settlement is still limited. For example, for L = 9 m at As = 35%, the difference between Ec 70 MPa and Ec 35 MPa only results in S = 0.271 – 0.272 m; whereas at As = 25%, S = 0.285 – 0.290 m. The small difference confirms that the system's response is still dominated by the punching mechanism, where much of the load is transmitted from the column tip to the soft soil below, so that increases in column stiffness or density have not been optimally mobilized (Fig. 3).

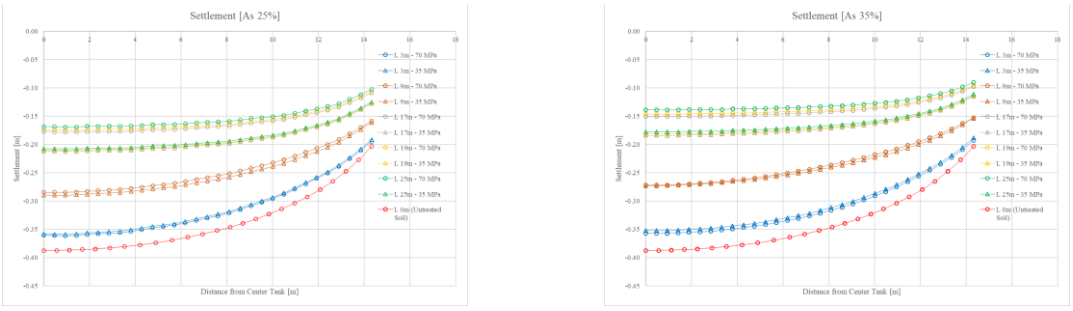

(a) (b)

Fig. 3. Settlement Improved Soil (a) Area Replacement Ratio 25% and (b) Area Replacemetn Ratio 35%
Source: Anlysis Results

Conversely, after the column penetrates the soft layer (L ≥ 17 m), there is a performance jump reflected in a much smaller decrease and higher sensitivity to As and Ec (Fig. 3). At As = 35% with Ec = 70 MPa, the decrease drops from 0.151 m (L = 17 m) to 0.147 m (L = 19 m) and 0.139 m (L = 25 m). For As = 25% and Ec = 70 MPa, the reductions are 0.179 m (L = 17 m), 0.175 m (L = 19 m), and 0.169 m (L = 25 m). The difference between Ec 70 MPa and Ec 35 MPa at L = 19 m reaches = 0.036 m at As 25% and = 0.035 m at As 35%, confirming that column stiffness and density (As) become the primary factors after penetration is achieved.

The effectiveness of the improvement is summarized by the Settlement Improvement Factor (SIF) = S_0/S (Table 2; Fig. 4). At As = 25%, the SIF increases from 1.36 (L = 9 m, Ec 70 MPa) to 2.29 (L = 25 m, Ec 70 MPa); at Ec 35 MPa, it rises from 1.34 to 1.86 for L = 9 → 25 m. At As = 35%, the increase is more pronounced: 2.565 (L = 17 m, Ec 70 MPa) → 2.642 (L = 19 m) → 2.786 (L = 25 m); at Ec 35 MPa: 2.105 (L = 17 m) → 2.130 (L = 19 m) → 2.176 (L = 25 m). The optimal configuration of the study was obtained at L = 25 m, As = 35%, Ec = 70 MPa with S = 0.139 m (SIF = 2.786, reduction ~64%), while the service threshold S ≤ 0.15 m is already met at L = 19 m for As = 35%, Ec = 70 MPa.

Table 2: Settlement Improvement Factor for Area Replacement Ratio 25%

L	Area Replacement Ratio 25%				Area Replacement Ratio 35%			
	Ec 70 MPa		Ec 35 MPa		Ec 70 MPa		Ec 35 MPa	
	ΔS	SIF	ΔS	SIF	ΔS	SIF	ΔS	SIF
[m]	[m]	[-]	[m]	[-]	[m]	[-]	[m]	[-]
0	0.388	1.000	0.388	1.000	0.388	1.000	0.388	1.000
3	0.362	1.071	0.359	1.080	0.357	1.085	0.352	1.100
9	0.285	1.360	0.290	1.337	0.279	1.389	0.273	1.420
17	0.179	2.170	0.213	1.823	0.151	2.565	0.184	2.105
19	0.175	2.216	0.211	1.840	0.147	2.642	0.182	2.130
25	0.169	2.289	0.208	1.864	0.139	2.786	0.178	2.176

Source: Analysis Results

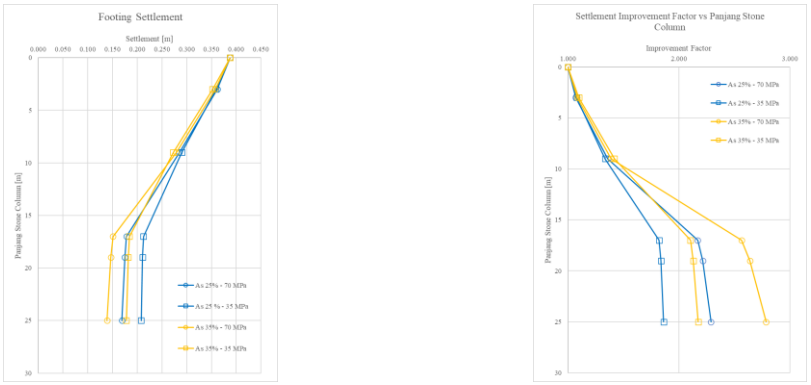

(a) (b)

Fig. 4. Settlement Improvement Factor for Various Parameter
Source: Analysis Results

These findings are qualitatively consistent with previous studies showing an increase in SIF with increasing column length and area ratio, but the absolute SIF values in this study are lower because the soft layer is much thicker (Hs = 17 m) compared to previous case (= 2 m), resulting in a smaller Hc/Hs ratio for the same column length. Compared to Priebe (1995), our numerical SIF values tend to lie below the theoretical curve $\varphi = 45°$ and approach $\varphi = 30–35°$ (Fig. 5), indicating a potential overestimate if the analytical method is applied without considering the thickness of the soft layer and the 3D group effect.

Practically, these results imply a design priority on selecting $L \geq Hs$ (17 m) to trigger a performance leap; thereafter, As and Ec are optimized to increase SIF while considering diminishing returns when L far exceeds Hs.

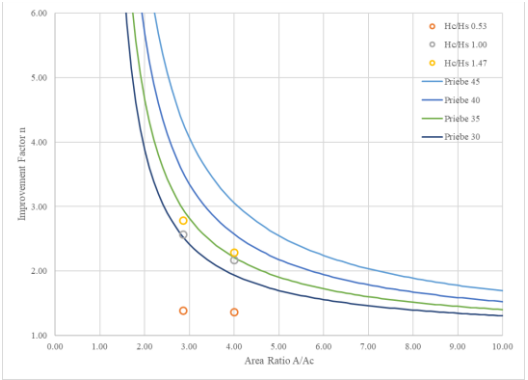

Fig. 5. Comparison of Settlement Improvement Factor Values with the Priebe Method (1995)
Source: Analysis Results

3.2. Deformation Patterns

Two indicators are used to diagnose the dominant deformation pattern, namely the punching ratio and compression ratio, which are calculated from displacement/strain according to the definition in the method. The reference for

determining the direction of deformation follows the displacement u scheme in Fig. 6 The calculation results are summarized in Table 3 and visualized in Fig. 7.

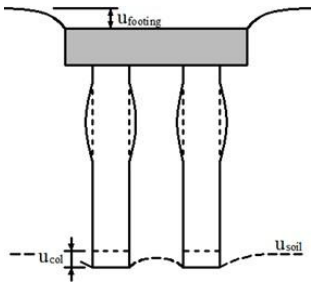

Fig. 6. Reference Displacement u in Deformation Pattern Analysis
Source: Killeen (2012)

Table 3: Punching and Compression Ratio for Various Parameter

L	Area Replacement Ratio 25%				Area Replacement Ratio 35%			
	As 25% - 70 MPa		As 25% - 35 MPa		As 25% - 70 MPa		As 25% - 35 MPa	
	Punching	Compression	Punching	Compression	Punching	Compression	Punching	Compression
[m]	[-]	[-]	[-]	[-]	[-]	[-]	[-]	[-]
3	0.037	0.048	0.032	0.069	0.025	0.048	0.023	0.064
9	0.048	0.260	0.045	0.259	0.037	0.248	0.034	0.264
17	0.025	0.604	0.029	0.491	0.025	0.434	0.018	0.579
19	0.010	0.652	0.009	0.551	0.011	0.487	0.006	0.630
25	0.008	0.756	0.006	0.681	0.010	0.625	0.004	0.746

Source: Analysis Results

In short columns (L < 17 m), deformation is dominated by punching. The punching ratio is relatively high, while the compression ratio is still low. For example, for L = 9 m at As = 25%, the punching ratio is approximately 0.048 (Ec = 70 MPa) and approximately 0.045 (Ec = 35 MPa) with a compression ratio of approximately 0.260 – 0.259 (Table 3). This pattern indicates that the load from the tank base is still largely transmitted directly to the soft soil beneath the column tip, so that increases in column stiffness (Ec) or column density (As) have not been fully mobilized.

(a) (b)

Fig. 7. Analysis Results of (a) Punching Ratio and (b) Compression Ratio
Source: Analysis Results

When L ≥ 17 m (the column penetrates the soft layer), the mechanism shifts toward bulging at the top of the column. The punching ratio decreases sharply (e.g., at L = 25 m: 0.008 – 0.010), while the compression ratio increases significantly (e.g., As = 25%, Ec = 70 MPa: 0.756; As = 35%, Ec = 70 MPa: 0.625). At the transition condition L = 17 m, both mechanisms coexist – for example, As = 35%, Ec = 70 MPa yields a punching ratio = 0.025 and compression ratio = 0.434 – but the contribution of radial deformation (bulging) begins to dominate.

The effect of As becomes apparent once penetration is achieved. In the stiff column (Ec = 70 MPa), an increase in As (25% → 35%) reduces the compression ratio (e.g., L = 25 m: 0.756 → 0.625), indicating improved lateral restraint due to closer column spacing, thereby reducing radial expansion. In softer columns (Ec = 35 MPa), this trend is less pronounced, and some combinations still exhibit high compression ratios, limiting the benefits of increasing As without corresponding increases in Ec.

This deformation pattern aligns with the settlement behavior discussed earlier: punching dominance at L < 17 m is associated with significant settlement and low SIF, while bulging dominance at L > 17 m is associated with minimal settlement and high SIF due to load distribution being more evenly distributed through column side friction and support from stiffer soil layers. Practically, these results emphasize the importance of achieving L ≥ Hs to shift the deformation mode from punching to bulging, thereby optimizing the performance of the reinforcement.

3.3. Stress Distribution

The results of mapping the effective vertical stress on the surface at the base of the LTP (Fig. 8) show stress peaks that coincide with the position of the stone columns and stress valleys in the inter-column zone. This pattern confirms the load sharing mechanism, in which the columns – as more rigid elements – attract a larger portion of the load than the surrounding soil. Increasing the replacement ratio area from 25% to 35% makes the columns' contribution more dominant: stress peaks above the columns tend to be higher, and the dispersion width (the transition zone from peak to valley) increases, resulting in a smoother stress gradient between column positions. The effects of column length (L) and column modulus (Ec) are also consistent; configurations with longer L (e.g., L = 25 m) and Ec = 70 MPa show higher stress peaks at the column head compared to shorter and/or softer columns.

The stress profile with respect to depth (Fig. 9) shows that σ'_v in the column increases from the head toward the depth and then changes sharply around the end of the column. At L = 25 m, the σ'_v value is relatively high to greater depths, indicating a more effective load transfer capacity to stiffer layers. At L = 17 – 19 m, the column's contribution remains significant above the column tip, but σ'_v in the column decreases rapidly below the tip – an indication that most of the load has been transferred to the supporting soil. The comparison of Ec = 35 and 70 MPa shows that stiffer columns consistently draw higher stresses throughout the depth, particularly in the upper third of the column, consistent with the dominance of the bulging mechanism in configurations that have penetrated soft layers.

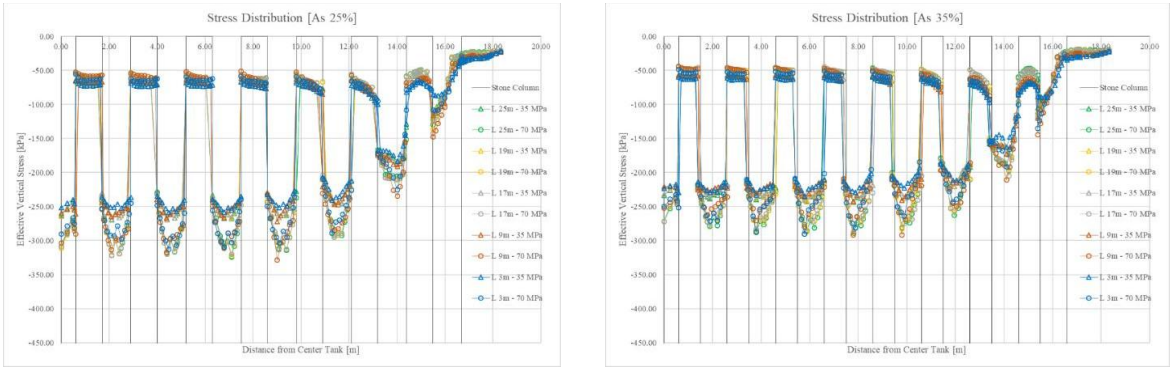

(a) (b)

Fig. 8. Stress Distribution of Stone Column (a) Area Replacement Ratio 25% and (b) Area Replacement Ratio 35%
Source: Analysis Results

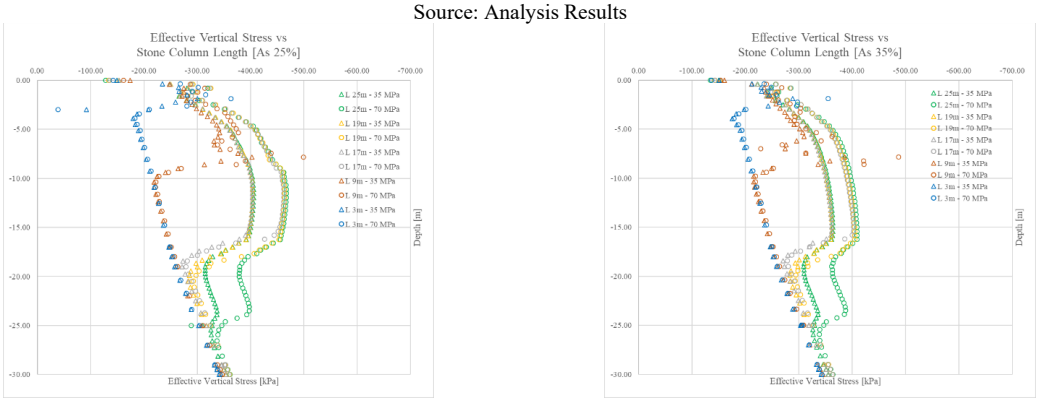

(a) (b)

Fig. 9. Stress Distribution of Stone Column Along Depth (a) Area Replacement Ratio 25% and (b) Area Replacement Ratio 35%

Source: Analysis Results

Overall, this stress distribution pattern is consistent with the settlement results: increases in As and Ec increase the portion of load borne by the columns and simultaneously widen the dispersion through the LTP, thereby decreasing the stress between columns. After L ≥ Hs (17 m), additional column length results in a peak stress increase that begins to saturate, but still contributes to improved differential settlement and SIF because the load is distributed more evenly to stiffer layers.

Stress Concentration Ratio

SCR = $\sigma'_{column}/\sigma'_{soil}$ is used to assess the proportion of load transferred to the column relative to the surrounding soil. The summary in Table 4 shows that all SCR values are > 3, with a range of = 3.46 – 5.35. This means that in all scenarios, the column always bears a greater vertical load than the surrounding soft soil – consistent with the stress peak pattern at the column location.

Effect of column stiffness (Ec). Increasing Ec from 35 to 70 MPa consistently increases SCR for all L and As. For example, at As = 25%, L = 9 m: SCR = 3.84 (Ec 35 MPa) becomes 5.01 (Ec 70 MPa); at L = 25 m: 3.65 → 4.82. A similar trend emerges at As = 35% (e.g., L = 19 m: 3.90 → 5.35), confirming that stiffer columns bear a larger portion of the load.

Effect of area replacement ratio (As). For the same Ec, As = 35% generally results in a higher SCR than As = 25%. For example, at Ec = 70 MPa, L = 17 m: SCR = 4.92 (As 25%) vs. 5.34 (As 35%); L = 19 m: 4.94 vs. 5.35. This aligns with greater load – sharing to the column network when column spacing is closer.

Effect of column length (L). For L < 17 m, SCR tends to increase with increasing L (e.g., As = 35%, Ec = 70 MPa: 4.60 (L = 3 m) → 5.15 (9 m)). Once penetration is achieved (L ≥ ~17 m), the SCR flattens out at approximately 5.3 ± 0.05 for Ec = 70 MPa and approximately 3.9 ± 0.2 for Ec = 35 MPa. This pattern is clearly visible in the distribution of Fig. 10 the highest values are at L = 17 – 19 m and decrease slightly/constantly as L is extended to 25 m.

Table 4: Stress Concentration Ratio for Various Parameter

L_{column}	Area Replacement Ratio 25%						Area Replacement Rati 35%					
	70 MPa			35 MPa			70 MPa			35 MPa		
	σ'_{1col}	σ'_{1soil}	SCF	σ'_{1col}	σ'_{1soil}	SCF	σ'_{1col}	σ'_{1soil}	SCF	σ'_{1col}	σ'_{1soil}	SCF
[m]	[kPa]	[kPa]	[-]	[kPa]	[kPa]	[-]	[kPa]	[kPa]	[-]	[kPa]	[kPa]	[-]
3	-277.95	-62.66	4.44	-245.58	-70.89	3.46	-242.91	-52.78	4.60	-222.28	-62.18	3.57
9	-287.19	-57.30	5.01	-255.99	-66.61	3.84	-245.00	-47.57	5.15	-222.03	-57.93	3.83
17	-289.73	-58.89	4.92	-253.51	-68.70	3.69	-250.83	-46.95	5.34	-226.69	-58.05	3.90
19	-290.24	-58.80	4.94	-253.36	-68.79	3.68	-251.26	-46.98	5.35	-226.58	-58.12	3.90
25	-287.50	-59.62	4.82	-252.17	-69.06	3.65	-252.44	-47.58	5.31	-226.93	-58.39	3.89

Source: Analysis Results

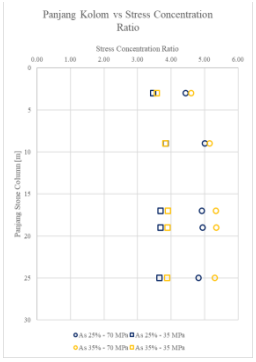

Fig. 10. Stone Column Length vs Stress Concentration Ratio
Source: Analysis Results

Mechanistically, the increase in SCR at L < 17 m reflects the dominance of punching, where vertical stress is still concentrated on the column along the depth. When L penetrates the soft layer, lateral interaction (side friction/soil restraint) and bulging dominance reduce the average stress difference between the column and the soil at the bottom, so that SCR no longer increases significantly. This saturation pattern aligns with previous study findings.

The implication is that increasing Ec and As is effective for raising SCR (and consequently SIF), but the additional benefit of extending L above Hs (17 m) becomes limited. An efficient design should target L ≥ Hs, then optimize

As and Ec according to service and economic criteria..

3.4. Characteristic Column Behaviour

This synthesis summarizes the relationship between deformation patterns, stress distribution, load sharing, and settlement response in stone column (SC) + LTP systems. Three distinct behavioral modes are clearly identified from the combined Fig. 11, Fig. 12, and Fig. 13. First, the punching mode for short columns (L < 17 m); second, the transition mode when the column reaches the lower boundary of the soft layer (L = 17 m); and third, the bulging mode for long columns penetrating the soft layer (L > 17 m).

In punching mode (L = 9 m), the peak vertical and horizontal strains are localized at the column tip (Fig. 11 a – b). Stress concentration drops to a value of 1 immediately after passing the column tip (Fig. 11 c), indicating that the load is predominantly transferred to the soil layer below the column. Consistent with this, the punching ratio is relatively high (= 0.045 – 0.048) and the compression ratio remains low (= 0.259 – 0.260), resulting in a large S value (= 0.271 – 0.290 m) and a low SIF (= 1.34 – 1.39).

In the transition mode (L = 17 m), the peak lateral strain shifts to the upper – middle part of the column (Fig. 12 a – b). The punching ratio decreases (= 0.018 – 0.025) while the compression ratio increases (= 0.434 – 0.579). High SCR values are distributed throughout the depth with a peak in the upper zone (Fig. 12 c), indicating the onset of dominant bulging mechanisms and the formation of lateral load sharing to the surrounding soil. As a result, S decreases sharply and SIF surges (= 2.11 – 2.57), marking the threshold of behavioral change.

In the bulging mode (L = 25 m), the stiffer lower layer support minimizes column tip deformation. Vertical and horizontal strains become relatively uniform along the column body, peaking in the upper zone (Fig. 13 a – b). The punching ratio reaches = 0.008 – 0.010, and the compression ratio is high (= 0.625 – 0.756). The SCR remains large and stable throughout the depth (Fig. 13 c), consistent with the minimum S - the optimal configuration is L = 25 m, As = 35%, Ec = 70 MPa with S = 0.139 m and SIF = 2.786 (Table 2).

The effects of As and Ec moderate behavior across all three modes. Once penetration is achieved (L ≥ 17 m), As = 35% reduces the compression ratio compared to As = 25% (e.g., L = 25 m: 0.625 vs. 0.756), indicating increased lateral confinement due to closer column spacing. Increasing Ec (35 → 70 MPa) consistently increases the SCR at the column head, increasing the load – bearing capacity of the columns and smoothing the stress gradient between columns. The role of LTP (1 m) complements this mechanism by widening load dispersion and suppressing local differentials directly beneath the base.

Overall, the common thread in the system's behavior is the mechanistic path of punching → transition → bulging, which is controlled by the Hc/Hs ratio. Once L equals/exceeds Hs (17 m), the contributions of As and Ec become effective in increasing SCR and SIF while controlling the compression ratio. Above this threshold, the benefits of extending L show diminishing returns, so the most efficient design strategy is to target L ≥ Hs, then optimize As (= 30 – 35%) and Ec with LTP support to meet service criteria.

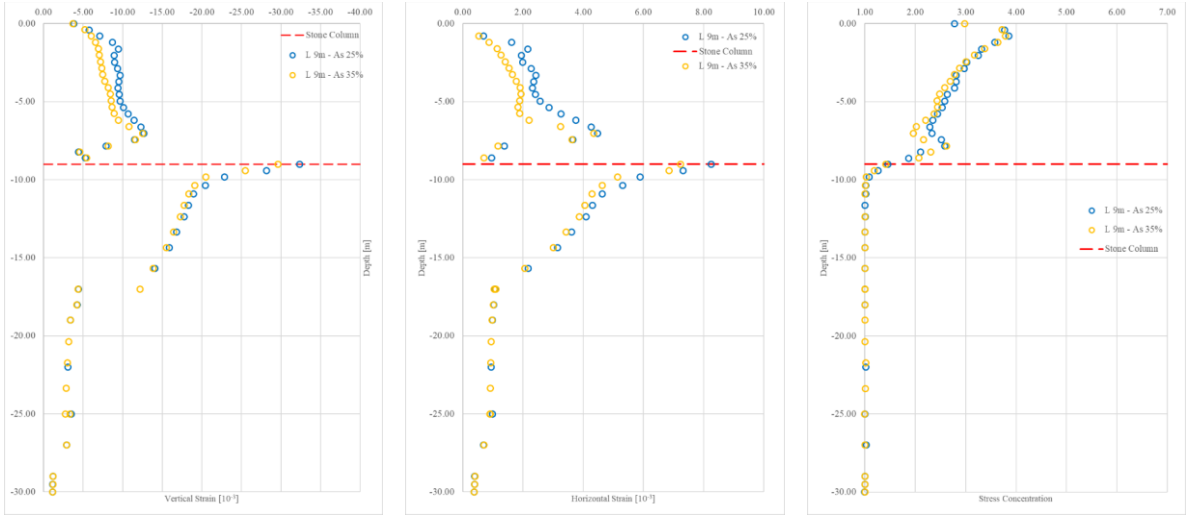

(a) (b) (c)

Fig. 11. Distribution of (a) Vertical Strain, (b) Horizontal Strain, and (c) Stress Concentration Ratio at a Stone Column Length of 9 m
Source: Analysis Results

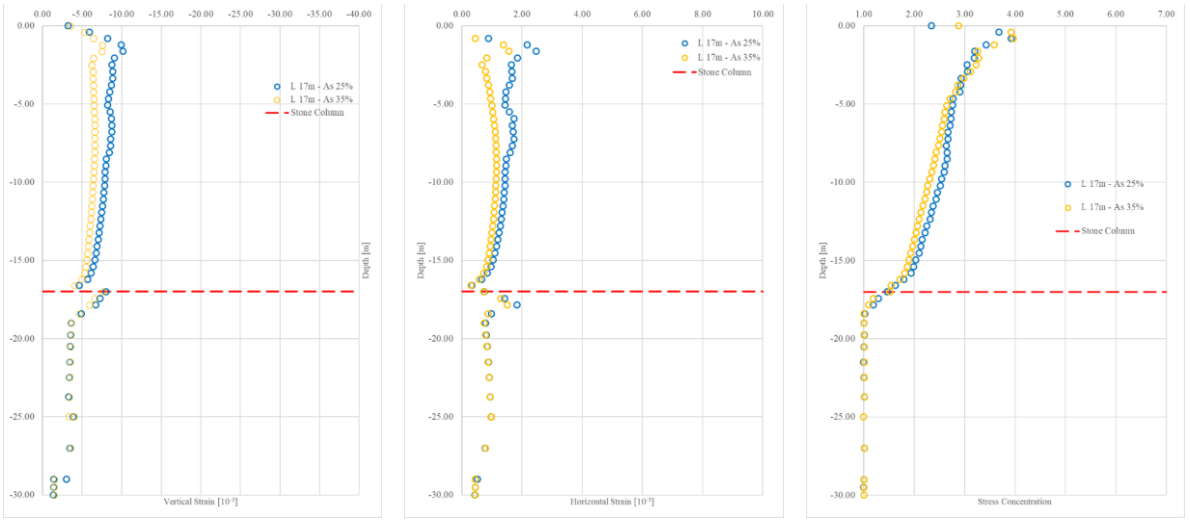

(a) (b) (c)

Fig. 12. Distribution of (a) Vertical Strain, (b) Horizontal Strain, and (c) Stress Concentration Ratio at a Stone Column Length of 17 m
Source: Analysis Results

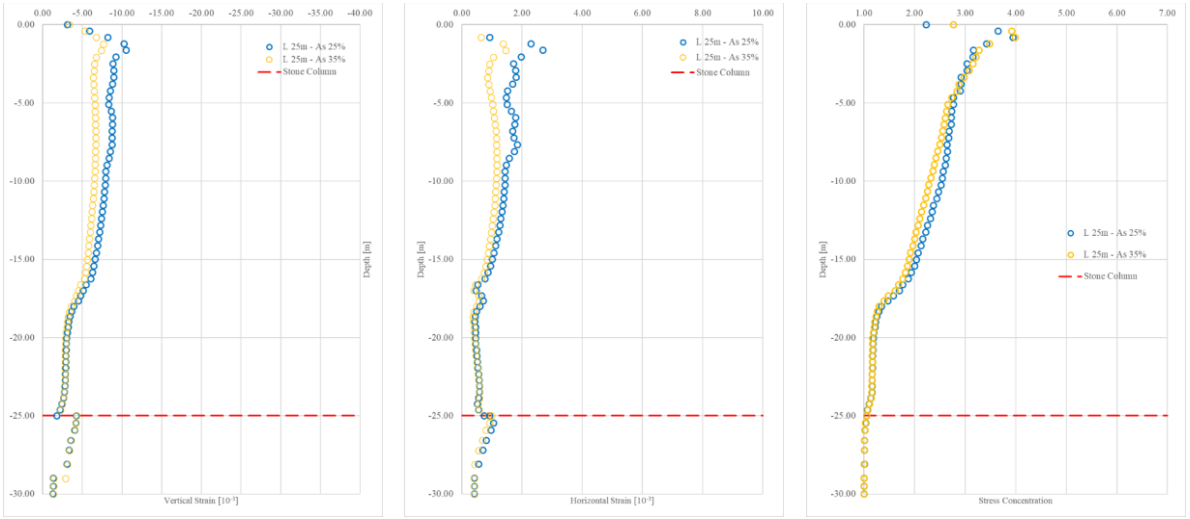

(a) (b) (c)

Fig. 13. Distribution of (a) Vertical Strain, (b) Horizontal Strain, and (c) Stress Concentration Ratio at a Stone Column Length of 17 m
Source: Analysis Results

4. Conclusions

Based on 3D numerical modeling and analysis of this case, the following key findings were obtained.

1. The stone column (SC) method is effective in reducing settlement with efficiency increasing with column length (L) – especially when L penetrates the entire thickness of the soft layer. A configuration meeting the service threshold $S \leq 0.15$ m is achieved at L = 19 m, As = 35%, and Ec = 70 MPa, with S = 0.147 m (SIF = 2.642, reduction = 62% from S_0 = 0.388 m). The success of the repair is determined not only by the properties of the column material but primarily by the Hc/Hs ratio, which enables optimal load sharing mobilization. Comparisons with Priebe (1995) and Killeen (2012) confirm that in thick soft layers, theoretical estimates require correction to avoid overestimation. The evaluation of the punching ratio and compression ratio reinforces the transition of deformation modes as L increases: L < 17 m is dominated by punching (transfer of vertical load to the column tip), L = 17 m shows a mixed mode, and L > 17 m is dominated by bulging (more even distribution of deformation along the column). An increase in As from 25% to 35% consistently decreases the compression ratio, indicating better lateral restraint against horizontal expansion of the column.
2. The effective vertical stress distribution shows stress peaks at the column position and valleys between columns, consistent with SCR values > 3 in all scenarios. For L < 17 m, the column–soil stress difference increases with increasing L (load concentration along the column, consistent with punching). When L ≥

17 m, stress at the bottom of the column decreases relatively while stress in the upper column – soil zone increases; horizontal strain in the upper zone indicates the dominance of bulging and lateral load transfer.

3. The three main performance control parameters are L, As, and Ec, with a hierarchy of influence depending on Hc/Hs. For L < 17 m, L becomes the main lever (an increase in L directly increases the load transfer capacity to the lower layer). After penetration (L ≥ 17 m), the influence of L decreases while As becomes the most significant lever in reducing settlement and differential settlement, followed by Ec, which increases the load portion on the column and smooths the stress gradient.

For future research, the following recommendations may be considered

1. For thick soft clay (Hs > 17 m), plan for a minimum L = Hs to trigger a performance jump; extensions far above Hs should be considered in light of diminishing returns and costs.
2. Use high Ec (≥ 70 MPa) and As ≥ 35% in heavy-load projects (e.g., tanks) to enhance lateral bearing capacity and more even load distribution, while minimizing differential settlement beneath the foundation.
3. Apply correction/reduction factors to empirical methods (e.g., Priebe, 1995) for thick Hs conditions or add 3D numerical verification to avoid overestimating results.
4. Conduct further numerical studies with a full – scale 3D model to explore the effects of column spacing, group patterns, and LTP configurations, as well as dynamic analysis (earthquake loads) on lateral deformation/liquefaction.

ACKNOWLEDGMENT

The author would like to thank Herwan Dermawan as the mentor for his guidance and input during the research. Thanks also go to Ardelia Luna for her support and assistance, as well as to friends who helped with discussions and simulations. Any shortcomings in this paper are entirely the responsibility of the author.

REFERENCES

1. Wardoyo , Sarwondo , Destiasari F, Wahyudin , Wiyono , Hasibuan G, et al. Atlas Sebaran Tanah Lunak Indonesia Bandung: Badan Geologi; 2019.
2. Terzaghi K, Peck RB. Mekanika Tanah dalam Praktek Rekayasa Jilid 1 Jakata: Erlangga; 1987.
3. Sekkelsten NH. Vibro Replacement - Sustainable Solution for Ground Improvement. Norwegia:; 2024.
4. Phung LD. Simplified FE-Simulation of Pile Installation Effect on Bearing Capacity of Displacement Piles in Sand. 2022.
5. Najjar SS. A State-of-the-Art Review of Stone/Sand-Column Reinforced Clay System. Springer. 2013.
6. Killeen M. Numerical Modelling of Small Group of Stone Column. Ireland:; 2012.
7. Han J. Principles and Practice of Ground Improvement Canada; 2015.
8. Das BM. Principle of Geotechnical Engineering 7th Edition USA: Cangage Learning; 2010.
9. Das BM, Sivakugan N. Principle of Foundation Engineering Ninth Edition Cengage Learning. Inc.; 2019.
10. Ameratunga J, Sivakugan N, Das BM. Soft Clay Engineering and Ground Improvement Oxon: CRC Press; 2021.
11. Ameratunga J, Sivakugan N, Das BM. Correlations of Soil and Rock Properties in Geotechnical Engineering India: Springer India 2016; 2016.
12. Alsirawan R. Analysis of Embankment Supportes by Rigid Inclusion Using Plaxis 3D. Acta Technica Jourinensis. 2021.
13. Abas HA, Medawi AM. Investigation stone column effectiveness for sabkha soil improvement: Field tests and numerical model. J. Umm Al-Qura Univ. Eng. Archit. 2024;: 67 - 77.
14. Look BG. Handbook of Geotechnical Investigation and Design Tables London: Taylor & Francis Group; 2007.